Photomagnetic positronium-spin conversion in phosphorescent solids*

Werner Brandt and Paul Kliauga†
Department of Physics, New York University, New York, New York 10003
(Received 5 November 1974)

Illumination affects the annihilation characteristics of positrons in positronium (Ps) forming phosphorescent substances, including photosynthetic materials *in vivo*. The excited triplet states T of the phosphors can induce Ps-spin conversion. The cross-section ratio of para-to-ortho Ps conversion and ortho-to-para Ps conversion is measured to be 9 ± 2. Two conversion processes which conserve total spin are considered. Spin catalysis converts Ps spin by electron exchange, leaving T unchanged. Spin flip converts Ps spin under the concomitant exothermic conversion of T to the singlet ground state. The experiments decide that spin flip dominates photomagnetic Ps-spin conversion.

I. INTRODUCTION

Following a first report,[1] this paper describes experiments which demonstrate the interaction of positrons with excited states of molecules. Changes in the lifetime spectra of positrons in photomagnetic solids are measured as a function of illumination in many phosphorescent substances, including some biological materials. The ratio of the cross sections for conversion of parapositronium, p-Ps (positron and electron spins antiparallel; spin quantum number $S=0$), to orthopositronium, o-Ps (positron and electron spins parallel; $S=1$), and for o-Ps to p-Ps is found to be 9 ± 2. This result implies that positronium-spin conversion on photoexcited molecular triplet states proceeds by a new process labeled spin flip, in which the excited triplet state converts to the singlet ground state.

Positrons annihilate in condensed matter with an electron predominantly into two γ quanta. The mean lifetime of free positrons is typically 0.5 nsec. In many insulators, positrons can capture an electron to form o-Ps and p-Ps in the ratio 3:1. Parapositronium annihilates into two γ quanta with a mean lifetime of 0.125 nsec. Orthopositronium *in vacuo* annihilates into three γ quanta with a lifetime of 140 nsec. In dense media, practically all positrons bound in o-Ps annihilate via fast paradecay with an electron bound in the medium into two γ quanta. The rate of such electron pick-off depends sensitively on the electron density of the medium, and usually gives lifetimes of 1–4 nsec. That is, positrons bound in o-Ps can be distinguished from positrons in other states in the positron lifetime spectra of Ps-forming substances.[2]

The existence of positronium was demonstrated by Deutsch and collaborators.[3] They detected the disappearance of o-Ps with addition of small amounts of the paramagnetic gases NO and O_2. Three mechanisms are known[4] to cause quenching of o-Ps: (i) Chemical reaction of Ps with molecules of the medium. (ii) Spin conversion to p-Ps through mixing of one magnetic substate of o-Ps with p-Ps in an external magnetic field. (iii) Spin conversion to p-Ps in interaction with ground-state paramagnetic impurities in the medium, such as free radicals and transition-metal ions. Parapositronium is converted by this mechanism into o-Ps with probability 3:1 relative to the o-Ps–to–p-Ps conversion. We present evidence for a process (iv) in which o-Ps and p-Ps undergo spin conversion via spin flip which quenches photoexcited molecules in metastable triplet states to their singlet ground states, where this Ps conversion probability is 9:1.

Phosphorescence of organic molecules was attributed by Jablonski[5] to the slow rate of emission of light in symmetry-forbidden transitions of the molecule in the lowest excited paramagnetic triplet state, T, to the diamagnetic singlet ground state (Fig. 1). His conjecture was proven to be correct by Lewis, Calvin, and Kasha.[6] When phosphor molecules are imbedded in rigid media, the phosphorescent lifetimes become so long that the steady-state concentration of triplet states under illumination makes the solid solutions paramagnetic. Photomagnetism is demonstrated through measurements of the paramagnetic susceptibility under illumination. Since then, phosphorescent states have been investigated extensively by electron spin resonance[7] and, in general, in the framework of exciton physics.[8]

We report on the interaction of Ps with photomagnetic molecules. Section II summarizes criteria for photomagnetic Ps-spin conversion. Section III describes the experiments, and Sec. IV gives the results. The analysis in Sec. V compares theory and experiment, leading to the conclusions summarized in Sec. VI.

II. CRITERIA FOR Ps SPIN CONVERSION

The longer lived of the two resolved positron-lifetime components is attributed to electron

pickoff by o-Ps. The short-lived component, then, comprises positrons that annihilate free, or bound in p-Ps and molecules. Positronium-spin conversion by excited triplet states can be measured through light-induced changes in the disappearance rate of the long-lived component, Γ_2, and in its intensity I_2, normalized such that $I_1+I_2=1$, where I_1 is the intensity from all other annihilation modes. A necessary consequence of o-Ps quenching by spin conversion is that Γ_2 and I_2 increase. Also, the conversion of o-Ps to p-Ps increases the narrow component and, hence, the pica (for "π-radian coincidence apparatus") count rate, I_P, at zero angle relative to 180° in the angular correlation between the two annihilation γ quanta. Conversion of p-Ps to o-Ps decreases I_P. On balance, I_P must increase under photomagnetic Ps-spin conversion, as delineated in Sec. V. Table I summarizes the experimental consequences of Ps-spin conversion and compares them to those of other mechanisms affecting Ps, such as Ps oxidation to a positron and inhibition of Ps formation.

Three-γ o-Ps disappearance rates are proportional to $I_2\Gamma_2^{-1}$.[9] Following Table I, both I_2 and Γ_2 should increase under illumination, and thus changes in the three-γ rate are uncharacteristic of Ps-spin conversion. Magnetic fields quench triplet states by mixing the magnetic $m=0$ sublevel and the singlet state with an efficiency proportional to the energy gap between the singlet and triplet states.[10] The energy gap between excited levels in phosphor molecules is ~0.1 eV, and between the ground states of o-Ps and p-Ps ~0.001 eV. Therefore, a magnetic field dependence of

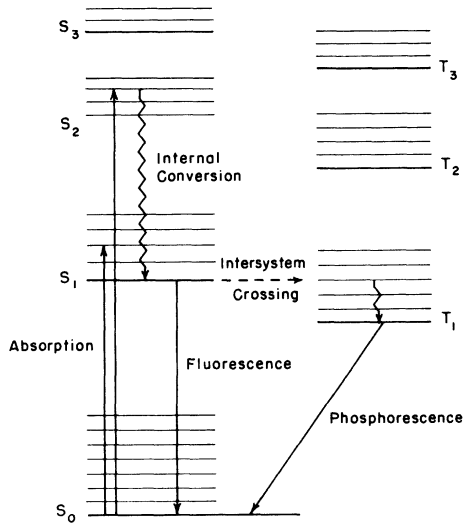

FIG. 1. Schematic energy-level diagram for a typical phosphor molecule (Jablonski diagram). Singlet states are labeled S_i (S_0 is the ground state), and triplet states are labeled T_i.

positron annihilation in photomagnetic substances can be indicative of Ps formation, but not of o-Ps interaction with a magnetic-field-dependent concentration of excited triplets.

We set minimum criteria for the assignment of changes in annihilation characteristics to Ps-spin conversion by light-excited triplets. (a) The samples must be diamagnetic in the dark. (b) Phosphors must exhibit a proper positron action spectrum in that only light absorbed by the phosphor molecules affects positron annihilation. (c) Light-induced changes must disappear at sample temperatures when thermal motion quenches the excited triplet states by internal conversion. (d) The changes must disappear if phosphorescent acidic (pH<7) solutions become fluorescent by making them alkaline (pH>7).

III. EXPERIMENTS

A. Apparatus

The positron-lifetime measurements were performed with a standard delayed-coincidence apparatus and ^{22}Na positron sources. The light-on and light-off lifetime spectra were stored concurrently. A routing pulse from the coincidence unit fed the input signals into one of the halves of a 400-channel pulse-height analyzer. A timed relay activated a shutter on the light source and switched the routing pulse from one half of the pulse-height analyzer to the other. The duration of the light-dark cycles in most experiments was set at 60 sec, long compared to the phosphorescence lifetimes (~2 sec), but short enough to avoid significant fluctuations in the sample temperature.

Limitations of sample photostability made high counting rates necessary. Without resorting to strong sources with their undesirable background, large scintillators (2×6 in.^{2} Naton plastic) were chosen at the sacrifice of resolution, which changed the full width at half-maximum in the prompt curve from 0.3 nsec with the normal 1×1 in.^{2} scintillators to 0.7 nsec. Still, the slope of the prompt curve, corresponding to 0.18 nsec,

TABLE I. Changes of positron annihilation characteristics induced through Ps quenching by different mechanisms. The symbols 0, +, and − denote no change, increase, and decrease, respectively, of the characteristic.

Annihilation characteristics	Ps-spin conversion	Ps oxidation	Ps inhibition
$\Delta\Gamma_2$	+	+	0
ΔI_2	+	+	−
ΔI_P	+	−	−

provided adequate resolution of the light-induced differences in the long lifetimes.

In geometry I, Fig. 2, the ^{22}Na source, in an envelope of 1.6-mg/cm^2 Al foil, was backed by a 3-mm-thick metal strip. This stopped all positrons not injected into the sample, contributing only to the short-lifetime component. In geometry II, light and positrons entered the sample through the same surface. As source substrates transparent to the phosphor-exciting light and with short positron lifetime, single crystals of LiF were chosen for the dyes, and single quartz crystals for the hydrocarbon solution, because the uv light produced defects in LiF giving an interfering long-lived positron component.

The light source, an Illumination Industries, Inc. 200 W super-pressure short-arc mercury lamp, was equipped with a spherical front-surface rear mirror and quartz lenses. Two 8-cm-thick water filters cooled the light by infrared absorption. A set of Corning glass filters selected spectral regions. The light intensity was varied by calibrated gray filters.

Absolute light intensities at the sample surface were determined with a SPEX double-beam spectrophotometer calibrated with a National Bureau of Standards source, and extrapolated to uv wavelengths with the spectral curves given by Parker.[11] The intensity was monitored with a Coherent Radiation Labs radiometer to correct for the aging of the lamp.

B. Phosphors

The boric acid solutions are solid at room temperature. The other solutions were measured as solid samples at low temperatures. Most measurements were taken at the boiling point of liquid nitrogen (77 °K). Before freezing, the solutions were degassed by standard freeze-thaw techniques.

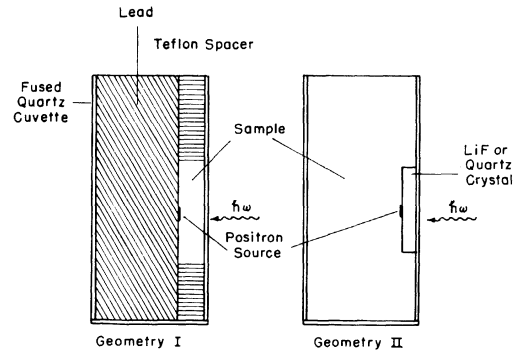

FIG. 2. Illustration of sample and positron source configurations in geometry I and geometry II.

Samples for geometry I were pipetted into a quartz cuvette with the positron source and its metal backing tied to one wall by a Teflon spacer, and frozen. The compressibility of the spacer and the nonuniformity of the source packet introduced an estimated uncertainty of ~0.1 mm in the thickness of the sample. This represents one of the largest sources of experimental uncertainty.

Samples for geometry II were prepared in the same manner, except that the crystal containing the ^{22}Na source was first affixed to the front surface of the cuvette by a thin layer of ethanol. When frozen slowly, this produced a clear ethanol glass transparent to the frequencies of interest.

The first columns in Table II list typical compositions of the photomagnetic materials investigated. Benzene and mesitylene were studied pure in the frozen polycrystalline state. Compositions *C*3 to *C*8 were standard reagent grade imbedded in polycrystalline matrices. Measurements showed that the light-induced changes were not affected by the degree of phosphor purity. Oil and water soluble chlorophylls (supplied by K+K Labs) gave the same light-induced positron-annihilation changes. The marine algae were grown in synthetic marine water exposed to sunlight.

The last group of samples had a glassy matrix of frozen glycerol (Matheson Coleman and Bell "Spectroquality," maximum water content 0.05%) or of boric acid (reagent grade, Kodak). During sample preparation, the glycerol was heated to 90 °C while bubbling dry nitrogen through the solution. The boric acid samples were prepared according to the instruction of Lewis, Calvin, and Kasha.[6] Rhodamine *B* was K+K Labs reagent; fluorescein was from British Drug House, Ltd. reagent grade. All samples were kept at 77 °K except where indicated.

In preliminary experiments, the effect of the stable free radical diphenyl-picryl-hydrazyl (DPPH) in benzene solutions on positron-lifetime spectra was studied. The DPPH (K+K Labs) concentrations were determined through absorption measurements in a Carey spectrophotometer.

C. Experimental uncertainties

The positron-lifetime spectra were resolved into two components by a least-squares-fit program based on a procedure by Cummings.[12] The statistical errors in Γ_2 are (2–3)%, in the Ps-spin conversion rates [equal to Γ_2(light-on) – Γ_2(light-off)] ~ 25%. In the intensities I_2 they are (5–10)%. By comparison, systematic instrumental errors were effectively eliminated through the light-on and light-off difference technique of alternating

TABLE II. Compositions and properties of photomagnetic materials. Phosphor preparations in crystalline matrices are denoted by C, in liquid matrices by L, and in glassy matrices by G. Columns give molecular phosphor density nC, sample thickness D, triplet formation efficiency ϕ_T, triplet lifetime τ_T, positron mass absorption coefficient α. The next-to-last two columns give the thickness dependence $e^{-\alpha D}$ and integrated light intensities appearing in Eqs. (24) and (25). Experiments were performed at 77°K unless indicated otherwise. The last column lists the volume rates for Ps propagation, ν, estimated with Eqs. (17), (24), and (25) from measured $\Delta\Gamma_2$ values listed in Table III.

Composition	Solute	Solvent	nC (10^{19} cm^{-3})	D (cm)	ϕ_T[a]	τ_T[a] (sec)	α (cm^{-1})	$e^{-\alpha D}$ (10^{-2})	$\int g_0(\bar{\nu})\,d\bar{\nu}$ (10^{15} photons cm^{-2} sec^{-1})	ν (cm^3 sec^{-1})
$C1$	benzene	•••	6.6(2)	0.15	0.8	3.0	36.9	0.39	3.9	1.2(−6)
$C2$	mesitylene[b]	•••	4.3(2)	•••	0.5?	1?	36.0	•••	0.02	9.4(−7)
$C3$	quinone	cyclohexane	1.5	0.23	0.5?	1?	32.7	0.05	3.9	4.1(−5)
$C4$	1, 2 bezanthracene	cyclohexane	1.8	0.23	0.8	1.0	32.7	0.05	3.9	5.4(−4)
$C5$	trans-stilbene	cyclohexane	1.2	0.23	0.5?	1?	32.7	0.05	3.9	2.0(−4)
$C6$	*bopq*[c]	cyclohexane	1.2	0.15	0.6?	5(−3)?	32.7	0.74	62	3.2(−5)
$C7$	chlorophyll	cyclohexane	2.4	0.15	0.24	4(−3)	32.7	0.74	320	1.9(−5)
$C8$	chlorophyll	ice	2.4	0.12	0.24	4(−3)	41.9	0.65	320	1.9(−5)
$L1$	marine algae[d,e]	water	•••	0.08	0.24	4(−3)	46.0	2.5	100	3.4(−6)
$L2$	marine algae[e,f]	water	•••	0.08	0.24	4(−3)	46.0	2.5	210	2.4(−6)
$G1$	rhodamine B	glycerol	8.4(−1)	0.08	0.3	2	52.8	1.5	210	1.0(−8)
$G2$	rhodamine B[b,d]	boric acid	1.6	•••	0.3	2	76.7	•••	0.25	3.9(−8)
$G3$	fluorescein	glycerol	7.2(−1)	0.08	0.85	2.5	52.8	1.5	190	3.2(−9)
$G4$	fluorescein[d]	boric acid	1.2	0.08	0.85	2.5	76.7	0.22	190	3.2(−9)

[a] From Ref. 11.
[b] Experiments performed with geometry II.
[c] Bis-butyloctyloxy-*p*-quaterphenyl.
[d] Room temperature.
[e] Blue filter (Corning CS 4-97).
[f] Yellow filter (Corning CS 3-71).

data storage.

Absolute values of the mean conversion rates depend sensitively on sample thickness, D, in geometry I, as $e^{-\alpha D}$ listed in Table II, where $\alpha \sim 50$ cm^{-1} is the positron mass absorption coefficient; D is of order 0.1 cm and known with only 10% accuracy. The evaluation of the light-absorption integral, listed in the last column of Table II, is afflicted by errors in the calibration of intensities and the numerical approximations used to evaluate the integral. We estimate the combined uncertainty from these causes to be ~25%.

In short, the compounded experimental uncertainties in the absolute determinations of lifetime differences between light on and off can be 50% or more. Of importance for judgments concerning the relation between theory and experiment are the systematic relative changes of these differences. They emerge with statistical significance from the body of our data in response to variations in experimental parameters such as light intensity and frequency, sample thickness, and temperature.

IV. RESULTS

A. Diphenyl-picryl-hydrazyl (DPPH)

As a test of our technique and of Table I, we measured the long-lived positron component in DPPH solutions with high statistical accuracy over a wider range of concentrations than reported heretofore,[4] with the results shown in Fig. 3. No indication is found up to 3% concentrations of a bending toward a saturation value equal to the spin-averaged Ps annihilation rate of 2 $nsec^{-1}$.[13] The intensity, I_2, decreases concommittantly and becomes indiscernibly small beyond 3%. The I_P count rate in the angular correlation decreases with increasing concentration.[14] By Table I, the solutions of DPPH molecules with stable unpaired electrons are an example of paramagnetic materials where o-Ps quenching is not dominated by Ps-spin conversion.

B. Photomagnetic Ps-spin conversion

Lifetime parameters of some phosphorescent solutions are tabulated in Table III. Changes in the phosphor concentrations, C, leave the annihilations in the dark unchanged. The difference $\Delta\Gamma_2 = \Gamma_2(\text{on}) - \Gamma_2(\text{off})$ is always positive. It is equal to the photoinduced o-Ps quenching rate, $\bar{\kappa}_o$, averaged over the volume sampled by the positrons. Figure 4 shows that $\bar{\kappa}_o$ increases linearly with the light intensity and, in geometry I, depends on D as $e^{-\alpha D}$. The lifetime spectra did not change under illumination if the frequency range of phosphor absorption was filtered out of the lamp spectrum. That is, the solutions exhibit the proper positron action spectrum.

Figure 5 illustrates that the quenching rate $\Delta\Gamma_2$ in a rhodamine-glycerol solution drops to zero above the glass temperature of glycerol, 190 °K, where phosphorescence ceases. The quenching rate in samples of fluorescein in ice did not change when made acid (pH < 7) by the addition of varying amounts of HCl before freezing. No effects of illumination could be observed when the solution was made basic (pH > 7) by the addition of NaOH.

Zero-angle count rates I_P of the angular correlations were measured for compositions $C1$, $C7$, $G1$, and $G3$; I_P always increased under illumination by a range of relative values

$$[I_P(\text{on}) - I_P(\text{off})]/I_P(\text{off}) = (5-10)\% \pm 3\% > 0 .$$

In summary, the photoinduced changes of positron-annihilation characteristics in the 33 phosphor samples investigated meet the criteria for photomagnetic Ps-spin conversion.

C. Photochromism

Photochromism refers to the reversible change of the visible absorption spectrum of substances

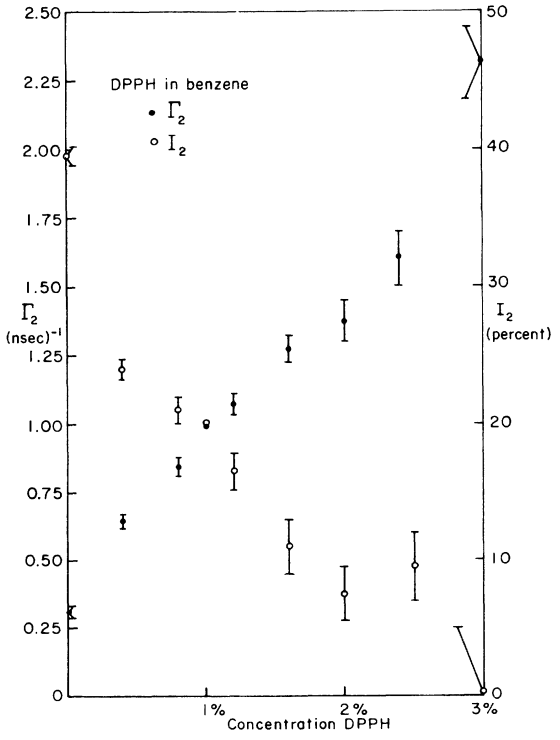

FIG. 3. Disappearance rate, Γ_2, and intensity, I_2, of the long-lived component as a function of concentration of DPPH in benzene.

induced by illumination. Photochromism can be stabilized by freezing a photochromic solution during illumination. Thermochromism refers to reversible changes in the visible absorption spectrum of a substance due to variations in temperature. Both phenomena are attributed to colored configurational isomers in singlet ground states.[15] Photochromism, in particular, should therefore not affect positron annihilation characteristics.

Solutions of bianthrone and its derivatives (2:2′-dimethyl-bianthrone and 2:2′-dibromobianthrone) were dissolved in ethanol and cooled to −100 °C to suppress irreversible photochemical changes which can occur at room temperature.[16] The photochromic isomer was prepared by illumination with the mercury lamp for 5 min. Sets of uncolored and photochromic solutions were stabilized in liquid nitrogen. Bianthrone is somewhat unusual in that it displays photochromism in its solid state, which is stable for weeks at room temperature.

Positron-lifetime spectra were measured for both sets, at 77 °K for the solutions and at room temperature for solid bianthrone, and found to be the same within statistical uncertainties.

D. Biological materials

Aqueous suspensions of marine algae and rhododendron leaves were investigated *in vivo* in geom-

TABLE III. Measured disappearance rates in μsec^{-1}, Γ_2(off), and intensities, I_2(off), of the long-lived component in the positron lifetime spectra in the dark, and their respective changes, $\Delta\Gamma_2$ and ΔI_2, under illumination. The statistical errors quoted in parantheses are calculated by a least-squares curve-fitting program. By Eq. (15), Γ_2(off) is identified with γ_o, the o-Ps pickoff rate in the solvent, and $\Delta\Gamma_2$ with $\bar{\kappa}_o$, the mean ortho-to-para Ps photomagnetic conversion rate. The symbols in the first column refer to the compositions listed in Table II. Small letters label samples made of the same solute and solvent but prepared under various conditions. The data are displayed in Fig. 6 where Y is the numerator and X the denominator of Eq. (26). The ratios α_p/α_o as calculated from the data by Eq. (26) are listed in the last column.

Composition	Γ_2(off)	$\Delta\Gamma_2$	I_2(off)	ΔI_2	α_p/α_o
*C*1	916(30)	158(43)	0.101(0.007)	0.036(0.011)	12
*C*1*a*	938(24)	109(36)	0.128(0.008)	0.033(0.012)	13
*C*1*b*	1013(23)	18(33)	0.143(0.007)	0.005(0.010)	10
*C*1*c*	885(22)	72(32)	0.119(0.005)	0.010(0.007)	6
*C*1*d*	929(22)	38(33)	0.130(0.006)	0.011(0.009)	12
*C*1*e*	882(21)	79(34)	0.120(0.006)	0.013(0.009)	7
*C*1*f*	879(18)	77(29)	0.120(0.007)	0.015(0.010)	9
*C*1*g*	867(17)	68(27)	0.113(0.006)	0.018(0.009)	13
*C*1*h*	965(20)	27(29)	0.144(0.007)	0.007(0.010)	9
*C*1*i*	973(22)	42(31)	0.137(0.008)	0.015(0.011)	14
*C*1*j*	876(20)	59(30)	0.101(0.008)	0.011(0.010)	10
*C*1*k*	870(18)	75(28)	0.107(0.007)	0.015(0.011)	10
*C*1*l*	1065(30)	64(43)	0.129(0.006)	0.009(0.009)	6
*C*1*m*	887(25)	124(37)	0.099(0.005)	0.020(0.007)	9
*C*2	629(30)	34(42)	0.172(0.007)	0.012(0.010)	11
*C*3	615(22)	131(31)	0.067(0.005)	0.009(0.007)	6
*C*4	767(15)	55(22)	0.090(0.004)	0.008(0.006)	9
*C*5	627(21)	29(30)	0.081(0.005)	0.004(0.007)	9
*C*6	577(21)	144(32)	0.075(0.005)	0.016(0.007)	8
*C*7	723(30)	138(42)	0.110(0.006)	0.010(0.009)	4
*C*8	595(21)	156(30)	0.063(0.005)	0.015(0.008)	9
*L*1	554(15)	37(21)	0.215(0.006)	0.017(0.010)	12
*L*2	511(15)	47(22)	0.185(0.005)	0.019(0.007)	12
*G*1	855(31)	103(47)	0.087(0.007)	0.013(0.010)	8
*G*1*a*	894(30)	86(45)	0.085(0.006)	0.010(0.009)	7
*G*1*b*	878(30)	128(45)	0.129(0.007)	0.040(0.011)	13
*G*1*c*	876(31)	86(44)	0.127(0.008)	0.032(0.012)	16
*G*1*d*	894(26)	58(40)	0.104(0.006)	0.007(0.008)	6
*G*1*e*	899(28)	30(40)	0.106(0.007)	0.007(0.010)	12
*G*2	694(17)	45(25)	0.124(0.006)	0.004(0.008)	4
*G*3	988(36)	103(53)	0.124(0.011)	0.023(0.015)	10
*G*3*a*	995(36)	70(50)	0.124(0.008)	0.017(0.011)	10
*G*4	553(9)	22(13)	0.115(0.004)	0.005(0.006)	11

etry II. All experiments showed significant increases in Γ_2 and I_2. Two sets of data for marine algae are reported in Table III. No effect was observed with a green filter which transmits light between the two chlorophyll absorption peaks. A yellow filter (Corning CS 3-71) transparent at the low-frequency peak gave a 30% larger change in Γ_2 than a blue filter (Corning CS 4-97) centered near the high-frequency peak, consistent with the circumstance that the light intensity was ~50% larger in the yellow-red region than in the blue region. The results show the correct positron action spectrum of chlorophyll.

They leave the question open, however, whether the effects are caused by the excited chlorophyll triplet states or by the triplet–ground-state oxygen molecules produced during photosynthesis. Attempts to separate these two effects by "poisoning" the algae suspensions, which suppresses O_2 production by photosynthesis, failed because the poisoning procedure requires solutions too dilute for the positron method. Based on the analysis presented in Sec. V, our data on biological samples give indirect evidence that the preponderance of the photoinduced changes are attributable to the Ps-spin conversion by the excited triplet states of chlorophyll.

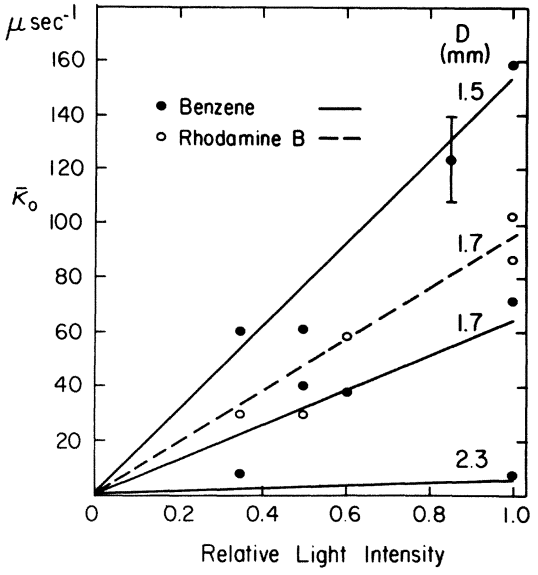

FIG. 4. Mean conversion rate $\bar{\kappa}_0$ vs light intensity, in geometry I (cf. Fig. 2). Slope varies with cell thickness as predicted by Eq. (24). Absolute value of $\bar{\kappa}_0$ can be uncertain by as much as 50%, but the relative uncertainties are comparable to the scatter about the theoretical lines. Solid points above the dashed line pertain to the upper solid curve, the others to the lower solid curve, and open symbols to the dashed line.

V. ANALYSIS

A. Lifetime spectra

Positrons from a ^{22}Na source are stopped in the sample with an implantation profile given to a good approximation by[17]

$$\delta P(x) = \alpha e^{-\alpha x}\,\delta x\,, \tag{1}$$

where $\alpha = 42d$ cm^{-1} is the mass absorption coefficient for ^{22}Na positrons in terms of the sample density d, in g cm^{-3}. Consider a layer of thickness δx at x so thin, $\alpha\delta \ll 1$, that the positron concentration can be treated as a constant. Let the Ps yield be β, the rate of o-Ps–to–p-Ps conversion at x be $\kappa_o(x)$, and the rate of p-Ps–to–o-Ps conversion be $\kappa_p(x)$. If $n_o(x,t)$ is the probability of an o-Ps atom formed at $t=0$ to survive until time t, and $n_p(x,t)$ is the corresponding quantity for p-Ps, one has

$$\dot{n}_o(x,t) = -\,[\gamma_o + \kappa_o(x)]n_o(x,t) + \kappa_p(x)n_p(x,t)\,, \tag{2}$$

$$\dot{n}_p(x,t) = -\,[\gamma_p + \kappa_p(x)]n_p(x,t) + \kappa_o(x)n_o(x,t)\,, \tag{3}$$

where γ_o is the rate of pickoff annihilation with no conversion and γ_p the self-annihilation rate of p-Ps. With the initial conditions

$$n_o(x,0) = \tfrac{3}{4}\beta\,,\quad n_p(x,0) = \tfrac{1}{4}\beta\,, \tag{4}$$

the solutions are

$$n_o(x,t) = \frac{3\beta}{4}\left(\frac{\Gamma_2(x) - \Gamma_o(x) + \frac{1}{3}\kappa_p(x)}{\Gamma_2(x) - \Gamma_1(x)}\,e^{-\Gamma_1(x)t} + \frac{\Gamma_1(x) - \Gamma_o(x) + \frac{1}{3}\kappa_p(x)}{\Gamma_1(x) - \Gamma_2(x)}\,e^{-\Gamma_2(x)t}\right) \tag{5}$$

and

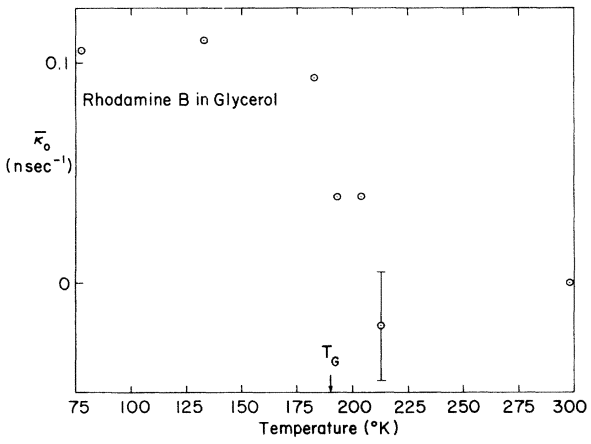

FIG. 5. Temperature dependence of the mean conversion rate $\bar{\kappa}_0$ for rhodamine B in glycerol. Glass transformation temperature of glycerol is denoted by T_G (~190°K).

$$n_p(x,t)=\frac{\beta}{4}\left(\frac{\Gamma_2(x)-\Gamma_p(x)+3\kappa_o(x)}{\Gamma_2(x)-\Gamma_1(x)}e^{-\Gamma_1(x)t}\right.$$

$$\left.+\frac{\Gamma_1(x)-\Gamma_p(x)+3\kappa_o(x)}{\Gamma_1(x)-\Gamma_2(x)}e^{-\Gamma_2(x)t}\right), \quad (6)$$

with the abbreviations $\Gamma_{o,p}(x)\equiv\gamma_{o,p}+\kappa_{o,p}(x)$. The disappearance rates are given by

$$\Gamma_{1,2}(x)=\tfrac{1}{2}[\gamma_p+\gamma_o+\kappa_p(x)+\kappa_o(x)$$
$$\pm(\{[\gamma_p+\kappa_p(x)]-[\gamma_o+\kappa_o(x)]\}^2$$
$$+4\kappa_o(x)\kappa_p(x))^{1/2}], \quad (7)$$

where the subscripts 1 and 2 refer to the "+" and "−" sign, respectively. In the limit $\kappa_{o,p}\ll\gamma_{o,p}$,

$$\Gamma_1(x)=\gamma_p+\kappa_p(x)\,,\quad \Gamma_2(x)=\gamma_o+\kappa_o(x)\,. \quad (8)$$

Combining Eqs. (5) and (6) yields the Ps-lifetime spectrum at x,

$$n_{\rm Ps}(x,t)=\beta[i_1(x)e^{-\Gamma_1(x)t}+i_2(x)e^{-\Gamma_2(x)t}]\,, \quad (9)$$

where

$$i_1(x)=\frac{\Gamma_2(x)-\gamma}{\Gamma_2(x)-\Gamma_1(x)},\quad i_2(x)=\frac{\Gamma_1(x)-\gamma}{\Gamma_1(x)-\Gamma_2(x)} \quad (10)$$

with the rate constant

$$\gamma=\tfrac{1}{4}\gamma_p+\tfrac{3}{4}\gamma_o\,. \quad (11)$$

In our experiments, one-half of the positrons are stopped in the source backing, where they annihilate with rate γ_c. The fraction $\frac{1}{2}(1-\beta)$ annihilates as free positrons in the sample, with rate γ_f. The fraction $\frac{1}{2}\beta$ annihilates as Ps with an x-dependent lifetime spectrum given by Eq. (9). The detectors average over the sample and, in geometry I, record the spectrum

$$n(t)=\frac{1}{2}\left(e^{-\gamma_c t}+(1-\beta)e^{-\gamma_f t}\right.$$
$$\left.+\beta\alpha\int_0^D n_{\rm Ps}(x,t)\,e^{-\alpha x}dx\right). \quad (12)$$

In geometry II, $n_{\rm Ps}(x,t)$ is replaced by $n_{\rm Ps}(D-x,t)$. The terms in Eq. (12) with rates $\ll\Gamma_2(x)$ are not resolved and appear as the short-lived component with mean disappearance rate $\overline{\Gamma}_1\simeq 3$ nsec^{-1} and intensity $I_1=1-I_2$. This component is dominated by light-insensitive annihilation channels and, as such, is of no further interest here.

Light-induced changes in the last term of Eq. (12) are the crux of our measurements. To leading terms pertinent to the lifetime ranges resolved in our experiments, one can write

$$n(t)=I_1e^{-\overline{\Gamma}_1 t}+I_2e^{-\Gamma_2 t}\,, \quad (13)$$

where the intensity $I_2=1-I_1$ is given by

$$I_2=\frac{\beta}{2}\,\frac{\Gamma_1-\gamma}{\Gamma_1-\Gamma_2} \quad (14)$$

in terms of the mean disappearance rates

$$\Gamma_1=\gamma_p+\overline{\kappa}_p\,;\quad \Gamma_2=\gamma_o+\overline{\kappa}_o\,, \quad (15)$$

which depend on the mean spin-conversion rates

$$\overline{\kappa}_{o,p}=\kappa^0_{o,p}\,f(\epsilon,\alpha,D)\,. \quad (16)$$

The function $f(\epsilon,\alpha,D)$ is a measure of the overlap between the positron implantation profile and the triplet concentration profile. The constants κ_p^0 and κ_o^0 are the conversion rates at the entrance surface for the light.

In general, the function $f(\epsilon,\alpha,D)$ cannot be given in analytical form. In the important ratio of conversion rates, κ_p/κ_o, this function cancels. To evaluate the conversion rates directly, we set

$$\kappa_p(x)=\alpha_p\nu nC_T(x);\quad \kappa_o(x)=\alpha_o\nu nC_T(x)\,, \quad (17)$$

where α_p is the probability for p-Ps spin conversion to o-Ps and α_o is the probability for o-Ps–spin conversion to p-Ps in interaction with molecules in triplet states, T, at a concentration $C_T(x)$; ν denotes the volume rate for the Ps-T interaction, and n is the molecular density in the sample. At the depth x, light of wave number $\overline{\nu}$ and intensity $I_0(\overline{\nu})$ maintains a steady-state concentration, $C_T(x,\overline{\nu})$, of randomly distributed triplet-excited molecules T. In the validity range of the Lambert-Beer law, C_T is given by

$$C_T(x,\overline{\nu})=C\,\frac{\phi_T\tau_T\epsilon(\overline{\nu})\,I_0(\overline{\nu})e^{-\epsilon(\overline{\nu})Cnx}}{1+\phi_T\tau_T\epsilon(\overline{\nu})\,I_0(\overline{\nu})e^{-\epsilon(\overline{\nu})Cnx}} \quad (18)$$

in geometry II. In geometry I, x has to be replaced by $D-x$. In Eq. (18), C denotes the concentration of phosphor molecules, ϕ_T is the triplet formation efficiency, τ_T is the triplet lifetime, and $\epsilon(\overline{\nu})$ is the photoabsorption cross section which is proportional to the usual extinction coefficient. Under our experimental conditions, the denominator in Eq. (18) can be set equal to 1. The overlap between the positron implantation profile [Eq. (1)] and the triplet concentration profile [Eq. (18)] can be evaluated with sufficient accuracy to obtain the function $f(\epsilon,\alpha,D)$ in the closed forms

$$f(\epsilon,\alpha,D)=\begin{cases}\dfrac{\alpha}{\epsilon Cn-\alpha}(e^{-\alpha D}-e^{-\epsilon CnD}) & \text{in geometry I} \quad (19)\\[2ex] \dfrac{\alpha}{\epsilon Cn+\alpha} & \text{in geometry II}\,. \quad (20)\end{cases}$$

We employed a light source with a wide frequency distribution $dI_0(\overline{\nu})/d\overline{\nu}\equiv g_0(\overline{\nu})$. The spin conversion rates must be integrated over the relevant absorption spectra of the phosphors, and $\Delta\Gamma_2$ becomes

$$\Delta\Gamma_2 = \bar{\kappa}_o = \alpha_o \nu n C \phi_T \tau_T \int f(\epsilon, \alpha, D)\, \epsilon(\bar{\nu})\, g_0(\bar{\nu})\, d\bar{\nu}\,. \tag{21}$$

If $\epsilon nC \gg \alpha$ in the frequency ranges of the phosphor absorption bands, Eqs. (19) and (20) simplify to

$$f(\epsilon, \alpha, D) = \begin{cases} \dfrac{\alpha}{\epsilon C n} e^{-\alpha D} & \text{in geometry I} \quad (22) \\ \dfrac{\alpha}{\epsilon C n} & \text{in geometry II}, \quad (23) \end{cases}$$

and Eq. (21) becomes

$$\Delta\Gamma_2 = \bar{\kappa}_o = \begin{cases} \alpha_o \nu \phi_T \tau_T \alpha e^{-\alpha D} \int g_0(\bar{\nu})\, d\bar{\nu} & \text{in geometry I} \quad (24) \\ \alpha_o \nu \phi_T \tau_T \alpha \int g_0(\bar{\nu})\, d\bar{\nu} & \text{in geometry II}, \quad (25) \end{cases}$$

where the integration extends over the phosphor absorption bands. That is, the mean conversion rates $\bar{\kappa}_p$ and $\bar{\kappa}_o$ are insensitive to the phosphor concentration C provided $\epsilon(\bar{\nu})nC \gg \alpha$ in the absorption bands leading to triplet formation, a condition fulfilled in our samples. The measured light absorption integrals appearing in Eqs. (24) and (25) are listed in Table II for typical experimental conditions.

When $\bar{\kappa}_p/\gamma_p \ll 1$ and $\bar{\kappa}_o/\gamma_o \ll 1$, one can approximate Eq. (14) as

$$I_2(\text{on}) = I_2(\text{off})[\Gamma_1(\text{on}) - \gamma]/[\Gamma_1(\text{off}) - \gamma]$$

and calculate, with Eqs. (11) and (15), the ratio of the spin conversion probabilities,

$$\frac{\alpha_p}{\alpha_o} = \frac{\bar{\kappa}_p}{\bar{\kappa}_o} \simeq \frac{3(\gamma_p - \gamma_o) I_2}{4 I_2 \Delta\Gamma_2}, \tag{26}$$

from the measured quantities $I_2 = I_2(\text{off})$, $\Delta I_2 \equiv I_2(\text{on}) - I_2(\text{off})$, $\Gamma_2(\text{off}) = \gamma_o$, $\Delta\Gamma_2 \equiv \Gamma_2(\text{on}) - \Gamma_2(\text{off})$, and the known p-Ps annihilation rate $\gamma_p = 8.0$ nsec^{-1}. In the early data analysis underlying Ref. 1, the value of γ_p was mistakenly set equal to the measured mean annihilation rate $\bar{\Gamma}_1 \simeq 3$ nsec^{-1}. This value is dictated by the source metal backing and, as such, irrelevant for the photomagnetic effects under investigation. Therefore, the ratios $\alpha_p/\alpha_o \simeq 2$ reported in Ref. 1 are in error. With the proper identification $\gamma_p = 8.0$ nsec^{-1}, one finds the values $\alpha_p/\alpha_o \simeq 9$ discussed in Sec. V C.

B. Narrow component

The p-Ps pendant to the o-Ps component annihilates predominantly by prompt 2γ decay. The annihilation quanta emerge from the sample essentially π rad apart because Ps is thermalized at the time of annihilation. The intensity of the resulting narrow component in the angular correlation curve is given by

$$F_N = \int_0^\infty \gamma_p n_p(t)\, dt\,, \tag{27}$$

where $n_p(t)$ is the probability that a Ps atom is in the para state at time t. Equation (6), after averaging over the sample, yields in the terms of Eq. (15):

$$F_N = \tfrac{1}{4}\beta\gamma_p(1/\Gamma_1 + 3\bar{\kappa}_0/\Gamma_1\Gamma_2)\,. \tag{28}$$

The intensity change of the narrow component under illumination is then given by

$$\frac{\Delta F_N}{F_N(\text{off})} = \frac{\bar{\kappa}_o[3\gamma_p - (\alpha_p/\alpha_o)\gamma_o]}{\gamma_o\gamma_p + \bar{\kappa}_o[\gamma_p + (\alpha_p/\alpha_o)\gamma_o]}\,, \tag{29}$$

where terms of second order in the conversion rates have been neglected. This change is always positive provided that $3\gamma_p > (\alpha_p/\alpha_o)\gamma_o$, as is the case in all our samples. In terms of the pica count rate, I_P, the fraction F_N is given by[17]

$$F_N = (I_P - I_{PW})/(I_{PN} - I_{PW})\,, \tag{30}$$

where I_{PN} and I_{PW} are the pica count rates if all positrons were to contribute to the narrow component or the wide component, respectively. The relative change for light-on and light-off, $\Delta I_P/I_P$, becomes

$$\frac{\Delta I_P}{I_P} = \frac{\Delta F_N}{F_N}\left(1 - \frac{I_{PW}}{I_P}\right). \tag{31}$$

Angular correlation data on Ps-forming solids show that, typically, $[1 - (I_{PW}/I_P)] \simeq 0.15$. From the lifetime data listed in Table III one calculates by Eq. (29) $\Delta F_N/F_N \simeq 0.2$–$0.4$ and, thus, predicts on the basis of Eq. (31) that $\Delta I_P/I_P \sim (3\text{–}6)\times 10^{-2} > 0$, in agreement with the experimental values of $\Delta I_P/I_P$ reported in Sec. IV B. They fulfill the condition listed in Table I for changes in I_P under illumination to be caused by photomagnetic Ps-spin conversion.

C. Spin statistics

Molecules in the lowest triplet state, T, and o-Ps atoms have three almost degenerate states with magnetic quantum numbers $m_S = 0, \pm 1$. The wave functions of the molecule, $\phi_S^{m_S}$ ($S=1$; $m_S = 0, \pm 1$), and of o-Ps, $\psi_S^{m_S}$ ($S=1$; $m_S = 0, \pm 1$), in terms of the usual spin basis functions $\alpha(\uparrow)$ and $\beta(\downarrow)$, take the form

$$\begin{aligned} &\phi_1^1 = \uparrow\uparrow, \quad \psi_1^1 = \uparrow\downarrow, \quad \phi_1^0 = 2^{-1/2}(\uparrow\downarrow + \downarrow\uparrow), \\ &\psi_1^0 = 2^{-1/2}(\uparrow\uparrow + \downarrow\downarrow), \quad \phi_1^{-1} = \downarrow\downarrow, \quad \psi_1^{-1} = \downarrow\uparrow. \end{aligned} \tag{32}$$

The positron spin function is denoted by $\uparrow$. The

molecule and p-Ps have singlet states with wave functions

$$\phi_0^0 = 2^{-1/2}(\uparrow\downarrow - \downarrow\uparrow), \quad \psi_0^0 = 2^{-1/2}(\uparrow\uparrow - \downarrow\downarrow). \tag{33}$$

As an example of an electron-exchange process we consider scattering in the substates ϕ_1^0 and ψ_1^1. The result is a "direct" interaction, or simple scattering, with amplitude D, or an electron exchange interaction, with amplitude E. All possible exchanges between each of the molecular electrons and the Ps electron yield

$$\begin{aligned}\phi_1^0\psi_1^1 = 2^{-1/2}(\uparrow\downarrow + \downarrow\uparrow)\uparrow\uparrow &\Rightarrow D\phi_1^0\psi_1^1 - (E/\sqrt{2})(\uparrow\uparrow\uparrow\uparrow + \downarrow\uparrow\uparrow\uparrow) \\ &+ (E/\sqrt{2})(\uparrow\uparrow\uparrow\uparrow + \uparrow\uparrow\downarrow\uparrow) \\ &= D\phi_1^0\psi_1^1 - E\phi_1^0\psi_1^1 + E\phi_1^1(\psi_1^0 - \psi_0^0) \\ &= (D-E)\phi_1^0\psi_1^1 + E\phi_1^1\psi_1^0 - E\phi_1^1\psi_0^0. \end{aligned} \tag{34}$$

The minus sign of the electron exchange amplitude E accounts for exchanges between electrons of identical spin orientation as required by the Pauli principle. The Ps spin state $\downarrow\uparrow$ after electron exchange is written as a linear combination of o-Ps and p-Ps spin eigenfunctions,

$$\downarrow\uparrow = 2^{-1/2}(\psi_1^0 - \psi_0^0). \tag{35}$$

Equation (34) implies: (a) Pure scattering, which leaves both T and o-Ps unchanged, proceeds by a direct process with amplitude D, and an electron exchange process with amplitude E. The coherent scattering amplitude is $D-E$, and the cross section becomes $(D-E)^2$. (b) Exchange interaction scatters both T and o-Ps into a different triplet sublevel, as given by the second term of Eq. (34), with amplitude E and cross section E^2. (c) Electron exchange also converts o-Ps into p-Ps as given by the third term, with amplitude $-E$ and cross section E^2; the molecular triplet wave function has not changed multiplicity, but has been scattered into a different magnetic sublevel. We label this process catalyzed Ps spin conversion.[18]

The same analysis is applied to each of the nine possible o-Ps$-T$ combinations, with the results given in Table IV. Inspection reveals that exchange scattering never leads to a final state in which the molecular triplet wave function has changed multiplicity. Positronium spin conversion by electron exchange proceeds only via catalysis.

The process of spin flip, in which Ps-spin conversion is accompanied by a change in the multiplicity of the molecular wave functions, is an allowed exothermic process for excited molecular states. It amounts to phosphorescence quenching through Ps-spin conversion. Spin-flip processes are enumerated in Table IV, with a scattering amplitude denoted by F and a cross section given by F^2. The combinations of spin functions are given pairwise to exhibit the possible electron exchange mechanisms. With appropriate Clebsch-Gordon coefficients in the phase convention of Condon and Shortley,[19] the nine possible normalized spin eigenfunctions of S^2 and m_S are listed in Table V.

The assumption that the total spin angular momentum is conserved requires that only eigenfunctions of the same total spin can appear on both sides of the scattering equation. Since the basis states in Table V are orthogonal, the cross sections can be deduced by inspection of Tables IV and V in terms of the sums of the squares of the scattering amplitudes quoted in Table VI. We see that the ratio α_p/α_o depends on the relative magnitudes of the amplitudes E and F. For $F=0$ we retrieve Ferrell's result $\alpha_p/\alpha_o = 3$ applicable to electron exchange with ground-state triplets and doublets.[13] For excited triplet molecules, α_p/α_o can range between 3 and 9, depending on the relative cross sections for catalytic electron exchange and for spin flip.

TABLE IV. Initial and final spin functions for exchange scattering (amplitude E) and spin flip (amplitude F). The amplitude for direct scattering is denoted by D. The molecular spin function is denoted by ϕ, the Ps spin functions by ψ. Superscripts give the values of m_S and subscripts the values of S. Here, ^{3}Ps denotes o-Ps and ^{1}Ps denotes p-Ps.

^{3}Ps → ^{1}Ps			^{1}Ps → ^{3}Ps		
Initial	Final	Amplitude	Initial	Final	Amplitude
$\phi_1^{\pm1}\psi_1^{\pm1}$	$\phi_1^{\pm1}\psi_1^{\pm1}$	$D-2E$			
	$\phi_1^0\psi_1^{\pm1}$	$D-E$		$\phi_1^{\pm1}\psi_0^0$	$D-E$
$\phi_1^0\psi_1^{\pm1}$	$\phi_1^{\pm1}\psi_1^0$	E	$\phi_1^{\pm1}\psi_0^0$	$\phi_1^0\psi_1^{\pm1}$	$-E$
	$\phi_1^{\pm1}\psi_0^0$	$\mp E$		$\phi_1^{\pm1}\psi_1^0$	$-E$
	$\phi_1^{\mp1}\psi_1^{\pm1}$	D		$\phi_1^0\psi_0^0$	$D-E$
$\phi_1^{\mp1}\psi_1^{\pm1}$	$\phi_1^0\psi_1^0$	E	$\phi_1^0\psi_0^0$	$\phi_1^1\psi_1^{-1}$	E
	$\phi_1^0\psi_0^0$	E		$\phi_1^{-1}\psi_1^1$	$-E$
	$\phi_1^{\pm1}\psi_1^0$	$D-E$	$\phi_1^{\pm1}\psi_0^0$	$\phi_1^{\pm1}\psi_0^0$	F
$\phi_1^{\pm1}\psi_1^0$	$\phi_1^0\psi_1^{\pm1}$	E	$\phi_1^0\psi_0^0$	$\phi_0^0\psi_1^1$	F
	$\phi_1^{\pm1}\psi_0^0$	$\pm E$			
	$\phi_1^0\psi_1^0$	$D-E$			
$\phi_1^0\psi_1^0$	$\phi_1^{-1}\psi_1^1$	E			
	$\phi_1^1\psi_1^{-1}$	E			
$\phi_1^{\pm1}\psi_1^{\mp1}$	$\phi_0^0\psi_0^0$	F			
$\phi_1^0\psi_1^0$	$\phi_0^0\psi_0^0$	F			

TABLE V. Eigenfunctions of S^2 and m_S for $S=2,1,0$ in terms of the combinations of spin functions ϕ and ψ listed in Table IV, with the notation $(+\,0)=\phi_1^1\psi_1^0$, $(-0)=\phi_1^{-1}\psi_1^0$, etc.

	S		
m_S	2	1	0
+2	(+ +)		
+1	$2^{-1/2}[(0+)+(+0)]$	$2^{-1/2}[(0+)-(+0)]$	
0	$6^{-1/2}[(-+)+(+-)]+(\sqrt{2}/\sqrt{3})$ (0 0)	$\frac{1}{2}[(-+)-(+-)]$	$3^{-1/2}[(-+)+(+-)]-3^{-1/2}$(0 0)
−1	$2^{-1/2}[(-0)+(0-)]$	$2^{-1/2}[(-0)-(0-)]$	
−2	(− −)		

Equation (26) permits us to determine α_p/α_o from the experimental data. Figure 6 displays the values of the numerator, Y, versus those of the denominator X, of Eq. (26), as calculated from the light-induced changes in the positron lifetime spectra of 33 phosphor solutions under a wide variety of experimental conditions as illustrated by the examples listed in Table III. The straight lines correspond to the three limiting values given in Table VI. Since the data points represent small differences of large numbers, they have large uncertainties, each of the order of the data scatter about the $\alpha_p/\alpha_o=9$ line. However, their distribution relative to that line is symmetrical with a width which defines an experimental slope $\alpha_p/\alpha_o=9\pm2$. The photosynthesizing phosphors fall in this range, and not near ~3 as it would be if the O_2 produced in photosynthesis was the Ps quencher. We conclude that spin flip dominates Ps spin conversion in photomagnetic substances.

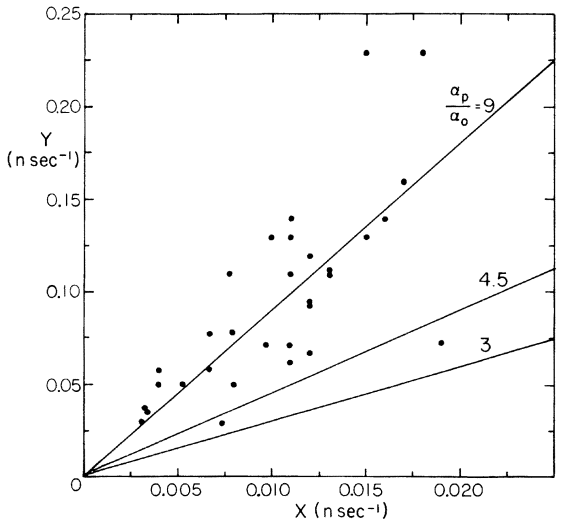

FIG. 6. Determination of $\alpha_p/\alpha_o=Y/X$, where Y is the numerator and X the denominator of Eq. (26). Lines are drawn for $Y/X=9$, 4.5, and 3, and represent the three limiting cases discussed in the text and Table VI. Relative uncertainty of points is comparable to the scatter of the data about the line $Y/X=9$. It is less than the separation between this line and $Y/X=4.5$.

D. Volume rates

We close with a comment about the volume rates for Ps spin conversion listed in the last column of Table III. They are estimated from Eqs. (24) and (25) under the assumption of spin interaction at each Ps-T collision, so that $\alpha_p\sim1$ and thus $\alpha_o\sim0.1$. Their magnitudes range from 10^{-5} to 10^{-6} cm^3/sec in the polycrystalline matrices to ~10^{-8} cm^3/sec in the glassy matrices. The results of a discussion about positron propagation given elsewhere[17] suggest that the former values are indicative of thermal Ps wave propagation in the polycrystalline van der Waals solids. The conversion rates are then limited by the Ps-T interaction cross sections in the range from 10 to 100 nm^2. This corresponds to interaction distances (2 to 6 nm)

TABLE VI. Positronium-spin-conversion processes between o-Ps (^{3}Ps) and p-Ps (^{1}Ps) and excited phosphor molecules in the triplet state ($^3M^*$) and the singlet state (^1M) via catalytic electron exchange (E) (the excited molecular triplet $^3M^*$ retains its multiplicity) and via spin flip (F) ($^3M^*$ converts to the singlet ground state ^1M).

Reactants	Mechanism	Products	Conversion cross section
^{3}Ps + $^3M^*$	exchange	^{1}Ps + $^3M^*$	$\frac{1}{3}E^2$
	spin flip	^{1}PS + ^1M	$\frac{1}{3}F^2$
^{1}Ps + $^3M^*$	exchange	^{3}Ps + $^3M^*$	E^2
	spin flip	^{3}Ps + ^1M	F^2

$\sigma_o\equiv\sigma_c$ (^{3}Ps → ^{1}Ps) = $\frac{1}{3}(E^2+\frac{1}{3}F^2)$

$\sigma_p\equiv\sigma_c$ (^{1}Ps → ^{3}Ps) = E^2+F^2

Thus,			
F^2/E^2	0	1	∞
$\sigma_p/\sigma_o=\alpha_p/\alpha_o$	3	$\frac{9}{2}$	9

comparable to the sum of the de Broglie wavelength of Ps ($\lambda_{Ps} \sim 12$ Å at 77 °K) and the size of the phosphor molecules (~10 Å). The lower values in amorphous matrices suggest that here spin conversion is limited by Ps diffusion, with diffusion constant $D_{Ps} \sim 0.01$ cm^2/sec.

VI. CONCLUSIONS

Illumination of phosphorescent solids changes positron annihilation characteristics in ways that are consistent with the tenet underlying this work that photoexcited molecular triplet states induce Ps spin conversion. The quantitative results select among possible spin conversion channels the process labeled spin flip in which the Ps spin converts under the concomittant deexcitation of the phosphor from the triplet state to the singlet groundstate. Photosynthesis *in vivo* is correlated with spin flip. Positronium conversion appears to be limited by the Ps-T scattering cross sections in polycrystalline van der Waals solids, and by Ps diffusion in amorphous molecular media.

ACKNOWLEDGMENT

We thank Kenneth Stanton for a critical reading of the manuscript.

---

*Work supported by the National Science Foundation.

†Present address: Dept. of Radiology, Columbia University College of Physicians and Surgeons, New York, N. Y. 10032.

[1]W. Brandt and P. Kliauga, Phys. Rev. Lett. 30, 354 (1973).

[2](a) For reviews see, e.g., *Positron Annihilation, 1965*, edited by A. T. Stewart and L. O. Roellig (Academic, New York, 1967); (b) *Proceedings of the Third International Conference on Positron Annihilation, Otaniemi, Finland, 1973*, edited by P. Hautojärvi and A. Seeger (Springer-Verlag, Berlin, 1975).

[3]J. W. Shearer and M. Deutsch, Phys. Rev. 76, 462 (1949).

[4]V. I. Goldanskii, At. Energy Rev. 6, 3 (1968); S. J. Tao and J. H. Green, J. Chem. Soc. A 82, 408 (1968).

[5]A. Jabloński, Z. Phys. 96, 236 (1935).

[6]G. N. Lewis, M. Calvin, and M. Kasha, J. Chem. Phys. 17, 804 (1949).

[7]C. A. Hutchison, Jr. and B. W. Mangum, J. Chem. Phys. 34, 908 (1961).

[8]For a recent review see J. B. Birks, *Photophysics of Aromatic Molecules* (Wiley-Interscience, New York, 1970).

[9]J. D. McGervey, in Ref. 2(a), p. 143ff.

[10]T. A. Pond and R. H. Dicke, Phys. Rev. 85, 489 (1952); V. L. Telegdi, J. C. Seno, D. D. Yovanovich, and S. D. Warshaw, Phys. Rev. 104, 867 (1956).

[11]C. A. Parker, *Photoluminescence of Solutions* (Elsevier, New York, 1968).

[12]J. B. Cummings, Brookhaven National Laboratory Report No. 6470, 1962 (unpublished).

[13]R. A. Ferrell, Phys. Rev. 110, 1355 (1958).

[14]R. L. de Zafra, Phys. Rev. 113, 1547 (1959).

[15]G. Kortüm and K. W. Koch, Chem. Ber. 100, 1515 (1967); L. A. Harrah and R. Becker, J. Phys. Chem. 69, 2487 (1967).

[16]H. Brockmann and R. Mühlmann, Chem. Ber. 82, 348 (1949).

[17]W. Brandt, Appl. Phys. 5, 1 (1974); and Ref. 2(b).

[18]G. Porter and M. Wright, Disc. Faraday Soc. 27, 18 (1959).

[19]E. U. Condon and G. H. Shortley, *The Theory of Atomic Spectra* (Cambridge U.P., London, 1935).